Neutron Density Distribution Deduced from Antiprotonic Atoms

A. Trzcińska for PS209 collaboration

Heavy Ion Laboratory, Warsaw University, PL-02-093 Warsaw, Poland

---

Antiprotons are a good probe for investigation of the nuclear surface due to the peripheral character of the $\overline{p}$-nucleus interaction. The PS209 experiment, performed at LEAR (CERN) aimed to study the nuclear periphery using antiprotons. Two experimental methods were applied.

The first method [1] is based on studying the radioactive residues of the antiproton annihilation process. The yields of products with one neutron less than target $N_t - 1$ (annihilation on a neutron) and one proton less than target $Z_t - 1$ (annihilation on a proton) were determined. Using these yields the halo factor (f_{halo}) was calculated [2–4] – the quantity related to the neutron to proton density ratio at distances about 2.5 fm larger than the charge half density radius [5].

The halo factors were compared with the results of the experiments determining the difference of the neutron and proton root mean square radii (Δr_{np}). The comparison indicates that neutron and proton distributions differ by the surface thickness rather than by the half density radius [6]. This means that the excess of neutrons is distributed in a form of a halo (not a skin).

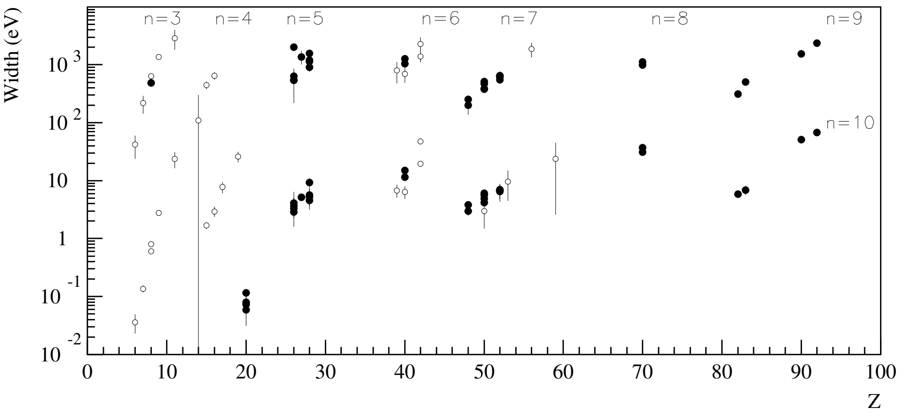

Fig. 1. Antiprotonic strong interaction level widths as a function of atomic number Z. Full circles – values determined in PS209 experiment; open circles – earlier data [7].

In the second experimental method applied antiprotonic x-rays were measured. The analysis of the spectra allows to determine antiprotonic level widths and shifts induced by the strong interactions. At present 44 levels shifts and 62 widths (for 34 isotopes) were determined (cf. Figure 1). The widths and shifts of the last levels depend on the strong interaction potential which to the first approximation is proportional to the nuclear matter density [8]. These observables, therefore, give information on the density at the nuclear periphery where the annihilation takes place.

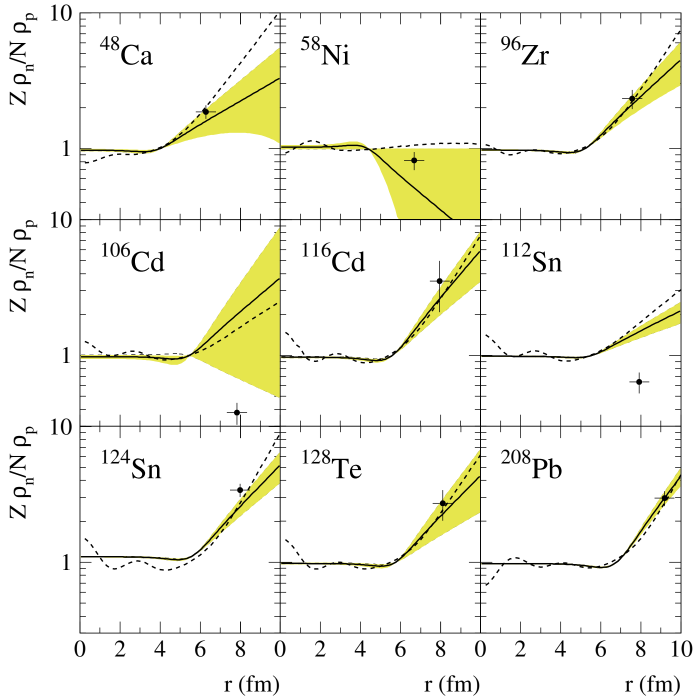

Fig. 2. Normalized neutron to proton density ratio $(Z \cdot \rho_n / N \cdot \rho_p)$ deduced from the strong-interaction level widths and shifts (solid lines with indicated statistical errors) and charge distributions given in Ref. [14] (Sn nuclei – see more explanation in Ref. [13]) and Ref. [15] (other nuclei). They are compared with f_{halo} measured in the radiochemical experiments (marked with crosses at a radial distance corresponding to the most probable annihilation site) and with the HFB model calculations [16] (dashed lines).

The details of the data analysis and a part of the results were reported in a number of articles [6,9–13]. The neutron density distributions were obtained from x-rays data using optical potential given in [8] (antiproton–nucleon scattering length equal $\overline{a} = (2.5 \pm 0.3) + i \cdot (3.4 \pm 0.3)$ fm), assuming two-parameter Fermi (2pF) density distributions and taking proton distribution from Refs. [14,15]. Figure 2 presents examples of the neutron to proton density ratios (neutron densities obtained from the x-ray data). The results are compared with the Hartree-Fock-Bogoliubov calculation [16] and the halo factor. A good agreement between the two experimental methods and theoretical predictions can be seen. The exceptions are ^{106}Cd and ^{112}Sn - the isotopes with

Table 1
Neutron and proton root mean square radii differences Δr_{np} obtained from antiprotonic x-ray data.

Isotope	Δr_{np} [fm]	Isotope	Δr_{np} [fm]	Isotope	Δr_{np} [fm]
^{40}Ca	$-0.08^{+0.05}_{-1.0}$	^{59}Co	$0.00^{+0.08}_{-0.13}$	^{122}Te	$0.08^{+0.04}_{-0.05}$
^{48}Ca	$0.09^{+0.05}_{-0.05}$	^{90}Zr	$0.09^{+0.02}_{-0.02}$	^{124}Te	$0.06^{+0.04}_{-0.04}$
^{54}Fe	$0.04^{+0.06}_{-0.08}$	^{96}Zr	$0.12^{+0.03}_{-0.03}$	^{126}Te	$0.11^{+0.03}_{-0.05}$
^{56}Fe	$0.03^{+0.08}_{-0.11}$	^{106}Cd	$0.10^{+0.10}_{-0.14}$	^{128}Te	$0.11^{+0.04}_{-0.05}$
^{57}Fe	$0.07^{+0.05}_{-0.05}$	^{116}Cd	$0.15^{+0.04}_{-0.04}$	^{130}Te	$0.15^{+0.06}_{-0.08}$
^{58}Ni	$-0.09^{+0.09}_{-0.16}$	^{112}Sn	$0.07^{+0.02}_{-0.02}$	^{208}Pb	$0.15^{+0.02}_{-0.02}$
^{60}Ni	$-0.01^{+0.08}_{-0.15}$	^{116}Sn	$0.10^{+0.03}_{-0.03}$	^{209}Bi	$0.18^{+0.04}_{-0.06}$
^{64}Ni	$0.04^{+0.07}_{-0.08}$	^{120}Sn	$0.08^{+0.03}_{-0.04}$	^{232}Th	$0.21^{+0.07}_{-0.07}$
		^{124}Sn	$0.14^{+0.03}_{-0.03}$	^{238}U	$0.21^{+0.07}_{-0.07}$

weakly bound protons. It was suggested [17] that this discrepancy may be explained by the creation of quasi-bound $\overline{\text{p}}$p states perturbing measurement of the halo factor.

Differences of neutron and proton root mean square radii Δr_{np} were determined from neutron density distributions obtained from strong interaction widths and shifts. Table 1 contains the results. (The values for Sn and Cd are slightly different from the ones presented in Ref. [6] as the corrections for the E2 resonance were introduced [13]). Data are also shown in the Figure 3 were Δr_{np} is plotted as a function of the assymetry parameter $\delta = (N - Z)/A$. The linear relationship was fitted: $\Delta r_{np} = (-0.03 \pm 0.02) + (0.90 \pm 0.15) \cdot \delta$ fm with χ^2 of 0.5.

Figure 4 shows theoretical predictions of Δr_{np} for even A isotopes obtained from HFB calculations. The data are compared with the fit for PS209 results. A fair agreement can be seen between experimental data and theoretical prediction for $\Delta r_{np}(\delta)$.

Antiprotonic atoms created from several isotopes of mass number ranging from 16 up to 238 were studied in the PS209 experiment. A rich set of data (halo factors, strong interaction widths and shifts) allowing study of nuclear surface was determined with a good precision. Neutron density distributions were deduced for several isotopes under the assumption of 2pF distribution. The results are in agreement with theoretical HFB model. Differences of neutron and proton root mean square radii Δr_{np} for isotopes of mass number ranging from 40 up to 238 were also determined. The relationship $\Delta r_{np}(\delta = (N-Z)/A)$ inferred from the experimental results is also consistent with a predictions of HFB calculations.

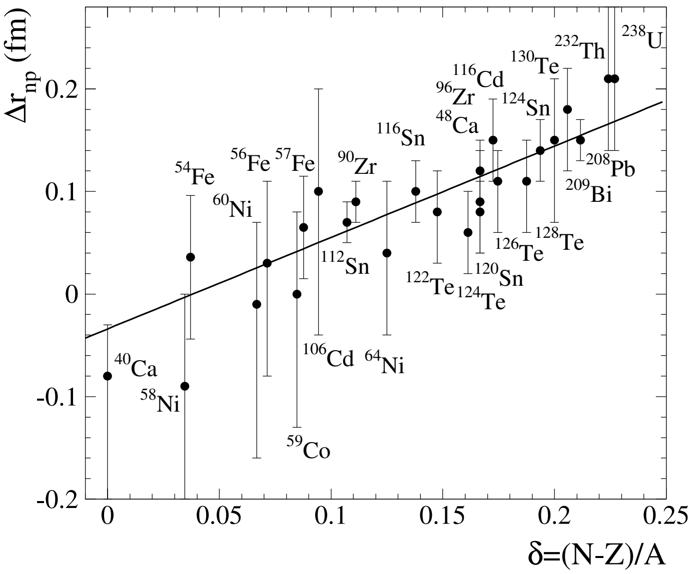

Fig. 3. Difference Δr_{np} between the rms radii of the neutron and proton distributions as deduced from the antiprotonic atom X-ray data, as a function of $\delta = (N-Z)/A$. The proton distributions were obtained from electron scattering data [14] (Sn nuclei) or from muonic atom data [15,18,19] (other nuclei). The full line represents the linear relationship between δ and Δr_{np} as obtained from a fit to the experimental data.

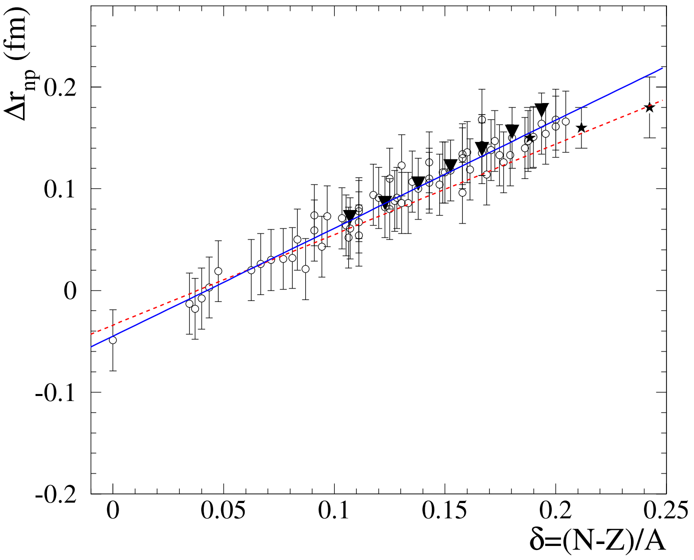

Fig. 4. Difference Δr_{np} between the rms radii of the neutron and proton distributions predicted by HFB (open points – [16], triangles – [20]) and HF (stars – [21]) calculations as a function of $\delta = (N-Z)/A$. The linear relationship $\Delta r_{np}(\delta)$ fitted to HFB [16] data ($\Delta r_{np} = (-0.05 \pm 0.01) + (1.06 \pm 0.08) \cdot \delta$ fm) – solid line and to PS209 data – dashed line are also shown.

Collected data provide rich material for the construction of the new, more sophisticated antiproton-nucleon optical potential [17,22,23].

It is considered to continue the studies of antiprotonic atoms. The proposed measurements include the search for odd-even effects in neutron distributions, the investigation of the abnormal upper level shifts as well as strong interaction effects on LS splitting in even nuclei. Also the investigation of the properties of deep levels via E2 resonance and search for the bound $\overline{\mathrm{p}}\mathrm{p}$ state effects in the x-rays are proposed. The experiment could be done at CERN using the ASACUSA facility.

References

[1] J. Jastrzębski et al., Nucl. Phys. **A558**, 405c (1993).

[2] P. Lubiński et al., Phys. Rev. Lett. **73**, 3199 (1994).

[3] P. Lubiński et al., Phys. Rev. C **57**, 2962 (1998).

[4] R. Schmidt et al., Phys. Rev. C **60**, 054309 (1999).

[5] S. Wycech et al., Phys. Rev. C **54**, 1832 (1996).

[6] A. Trzcińska et al. Phys. Rev. Lett. **87**,082501 (2001).

[7] C.J. Batty, E. Friedman, H.J. Gils, H. Rebel, in *Advances in Nuclear Physics.*

[8] C. J. Batty, E. Friedman, and A. Gal, Nucl. Phys. **A592**, 487 (1995).

[9] R. Schmidt et. al., Phys. Rev. C bf 58, 3195 (1998).

[10] A. Trzcińska et al. Nucl. Phys. A **692**,176c (2001).

[11] A. Trzcińska et al. Acta Phys. Pol. **32**, 917 (2001).

[12] J.F. Hartmann et al. Phys. Rev. C **65**, 014306 (2001).

[13] R. Schmidt et al. Phys. Rev. C, **67**, 044308 (2003).

[14] H. de Vries et al., At. Data Nucl. Data Tables, **36**, 495 (1987).

[15] G. Fricke et al, At. Data Nucl. Data Tables **60**, 177 (1995).

[16] R. Smolańczuk, private communication.

[17] S. Wycech Nucl. Phys. A **692**,29c (2001).

[18] J. D. Zumbro et al., Phys. Rev. Lett. **20**, 1888 (1984).

[19] J. D. Zumbro et al., Phys. Lett. **167B**, 383 (1986).

[20] F. Hofmann, H. Lenske, Phys. Rev. C 57 (1998) 2281.

[21] A. Brown, Phys. Rev. Lett. 85, 5296 (2000).

[22] S. Wycech, *Proceedings of LEAP2003 Conference*, Yokohama, 2003.

[23] E. Friedman, A. Gal, *Proceedings LEAP2003 Conference*, Yokohama, 2003.